J. Fluid Mech. (1968), *vol.* 34, *part* 3, *pp.* 497–515
Printed in Great Britain

Correlation measurements in grid turbulence using digital harmonic analysis

By C. W. VAN ATTA AND W. Y. CHEN

Department of the Aerospace and Mechanical Engineering Sciences and Institute for Pure and Applied Physical Sciences, University of California, San Diego, La Jolla, California

(Received 8 April 1968)

Two-point time correlations up to eighth order of longitudinal velocity fluctuations in grid-generated turbulence have been measured using linearized hot-wire anemometry, digital sampling, and a high-speed digital computer. A novel feature of the present measurements is the adoption of digital Fourier analysis, using the recently developed fast-Fourier transform method. The joint probability density function for the velocity fluctuations at two points separated in time is found to be significantly non-Gaussian. All measured even-order correlations are nearly identical with those reported by Frenkiel & Klebanoff (1967 *a*, *b*), and higher-order correlations may be accurately predicted from the second-order correlation by assuming a Gaussian joint probability density. All individual odd-order correlations are substantially different from those reported by Frenkiel & Klebanoff. In particular, all mean values of odd powers of the fluctuating velocity are nearly zero, and the correlations are nearly antisymmetrical functions of the time delay as would be the case for purely isotropic homogeneous turbulence. In spite of the large difference between the individual measured odd-order correlations and previous measurements, quantities such as the skewness and skewness factor derived from certain combinations of the correlations are found to be quite insensitive to observed differences in the form of the correlations and are very similar to previous measurements.

1. Introduction

In the course of a continuing experimental investigation of grid-generated turbulence, we have developed a method for very fast and efficient digital computer calculation of two-point correlations of arbitrary order. The heart of the method is the adoption of digital harmonic analysis, using the recently developed 'fast Fourier transform', an efficient scheme for obtaining the discrete Fourier transform of a time series of sampled data. The technique should prove useful for a variety of future measurements in turbulent flows. To date, two-point time correlations up to eighth order of the longitudinal fluctuating component of velocity at a single point in grid turbulence have been measured using linearized constant-temperature hot-wire anemometry and the discrete transform method. Other detailed measurements of these correlations, obtained by direct calculation of mean lagged products, have been reported recently by Frenkiel & Klebanoff (1967 *a*, *b*, hereinafter often referred to as I and II). Using constant-current hot-wire anemometry, they found that measurements of odd-order correlations required large corrections for the non-linear response of the hot wire. The corrections were frequently as large as the maximum values of the measured correlation functions. Corrections for the non-linear response were found to be negligible for even-order correlations. In the present measurements, constant-temperature, linearized hot-wire anemometry was used in order to avoid the necessity of such corrections.

Frenkiel & Klebanoff also found that a non-Gaussian joint-probability distribution of Gram–Charlier type described relations between their odd-order correlations fairly well, while the even-order correlations were related according to a Gaussian joint distribution, except for very small time separations.

The original goal of the present investigation was to obtain correlations up to only third order to study the dynamics of energy transfer in grid turbulence. This study is in progress. When the present third-order correlations were found to be significantly different from those of Frenkiel & Klebanoff, the measurements were extended to higher order to obtain a full comparison with previous results. Hence, all the higher correlations reported in I and II have been measured.

2. Experimental arrangement

The experiments were carried out in the 76 cm by 76 cm by 9 m test section of the low-turbulence wind tunnel in the Department of the Aerospace and Mechanical Engineering Sciences. Biplane grids of round, polished dural rods were located 2·4 m from the end of the contraction section. Two different grids were used, having mesh spacings M of 2·54 and 5·08 cm with rods of 0·477 and 0·953 cm diameter, respectively. The mean velocity U was 15·7 m/sec for the 2·54 cm grid measurements and 7·7 m/sec for the 5·08 cm grid measurements. The corresponding Reynolds numbers based on mesh spacing were 25,600 and 25,300 for the high- and low-speed data, respectively. The high-speed, small-grid experimental conditions were nearly identical with those of Frenkiel & Klebanoff (1967 *a*, *b*) with respect to grid geometry, mean velocity and x/M, where x is the distance downstream from the grid. Conventional analogue measurements of u and v, the longitudinal and transverse turbulent intensities, were made over a short range of x/M in the initial period of decay. As shown in figure 1, the decay of the velocity fluctuations in this range, when made appropriately dimensionless, is practically identical for both experimental conditions. The ratio $(\langle u^2\rangle/\langle v^2\rangle)^{\frac{1}{2}}$, a measure of the anisotropy of the turbulence, decreases as x/M increases, with an average value of 1·11 over the range $39 \leqslant x/M \leqslant 55$, about 2–3 % larger than reported by Comte-Bellot & Corrsin (1966) for comparable mesh Reynolds number, the same range of x/M, and the same type of grid.

All detailed digital measurements were made at $x/M = 48$. A tungsten hot wire, 1 mm long and 5μ in diameter was used to measure u, the longitudinal fluctuating component of the turbulent velocity field. A DISA 55 A 01 amplifier was used to operate the hot wire at constant resistance, with an overheat ratio of 0·5. The hot-wire output was linearized using a DISA 55 D 10 linearizer. The linearized hot-wire signal was FM tape recorded at a tape speed of 152·4 cm/sec using a Sanborn 3917 A recorder. The analogue tape was later played back and sampled with an analogue-to-digital converter at a rate somewhat faster than

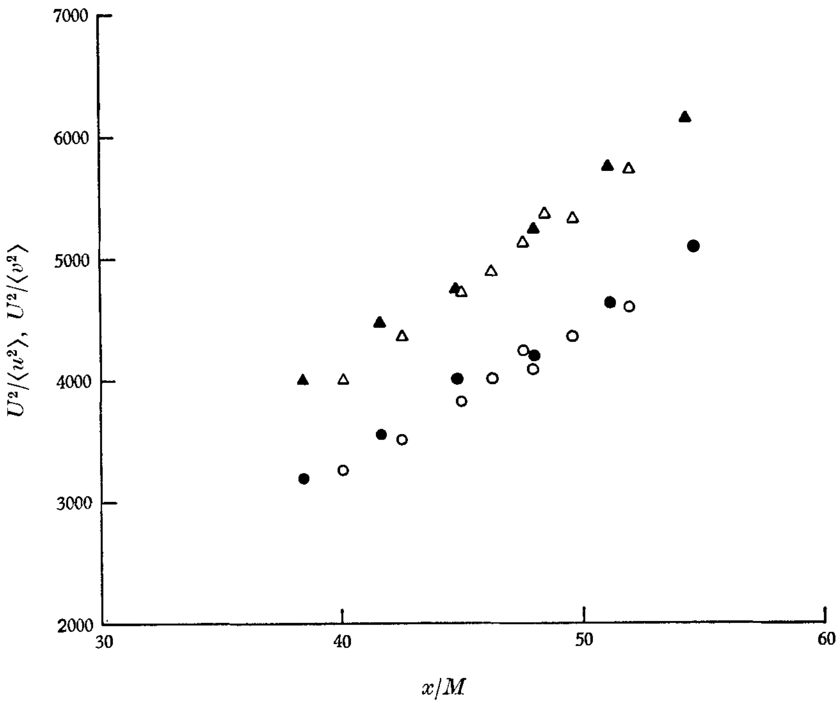

FIGURE 1. Decay of turbulent energy behind the two grids. M = 5·08 cm, U = 7·7 m/sec: ○, $U^2/\langle u^2\rangle$; △, $U^2/\langle v^2\rangle$. M = 2·54 cm, U = 15·7 m/sec: ●, $U^2/\langle u^2\rangle$; ▲, $U^2/\langle v^2\rangle$.

twice the highest frequency for which the turbulent spectrum was unmistakably distinguishable from electronic noise. This highest frequency was determined from a preliminary spectral analysis and was equal to 7 kHz and 1800 Hz for the 2·54 cm and 5·08 cm grid data, respectively. The corresponding sampling rates were 16,000 samples/sec and 5600 samples/sec.

The digital data were processed in several steps, using a CDC 3600 computer. As an initial step, the running mean values of $\langle u^2\rangle$ and $\langle u^3\rangle$ were computed to determine the amount of data necessary to provide stationary values of these quantities. Sampling time intervals of 25·6 and 54·9 sec were found to be adequate for the data at high and low speeds, respectively, and all subsequent averages were based on four samples of these lengths.

3. Distribution of velocity fluctuations

The one-dimensional probability densities $p(u/\sigma)$, where $\sigma = \langle u^2 \rangle^{\frac{1}{2}}$, were found to be closely Gaussian, as illustrated in figure 2. The joint probability density for the velocity taken at two different times

$$p[u(t)/\sigma,\ u(t+\tau)/\sigma] = p(v_1,\ v_2)$$

was found to be significantly non-Gaussian, as shown in figure 3. Here τ was chosen to correspond to a correlation coefficient of 0·686, the same as for the data used to compute the joint distribution for the longitudinal component of

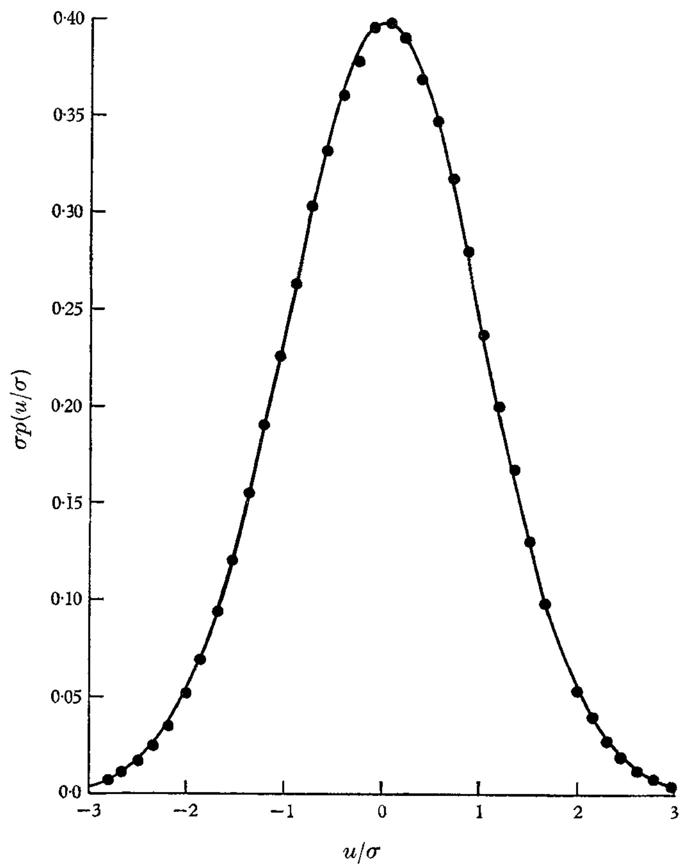

FIGURE 2. One-dimensional probability density for velocity fluctuations. M = 2·54 cm, U = 15·7 m/sec: solid line is Gaussian distribution.

velocity measured at two laterally separated points in grid turbulence by Frenkiel & Klebanoff (1965). The departures from Gaussianity are roughly the same as those found by Frenkiel & Klebanoff. The amount of scatter in the present data is somewhat smaller due to the larger number of velocity samples used to compute the probabilities (409,600 in the present case as compared with 160,020).

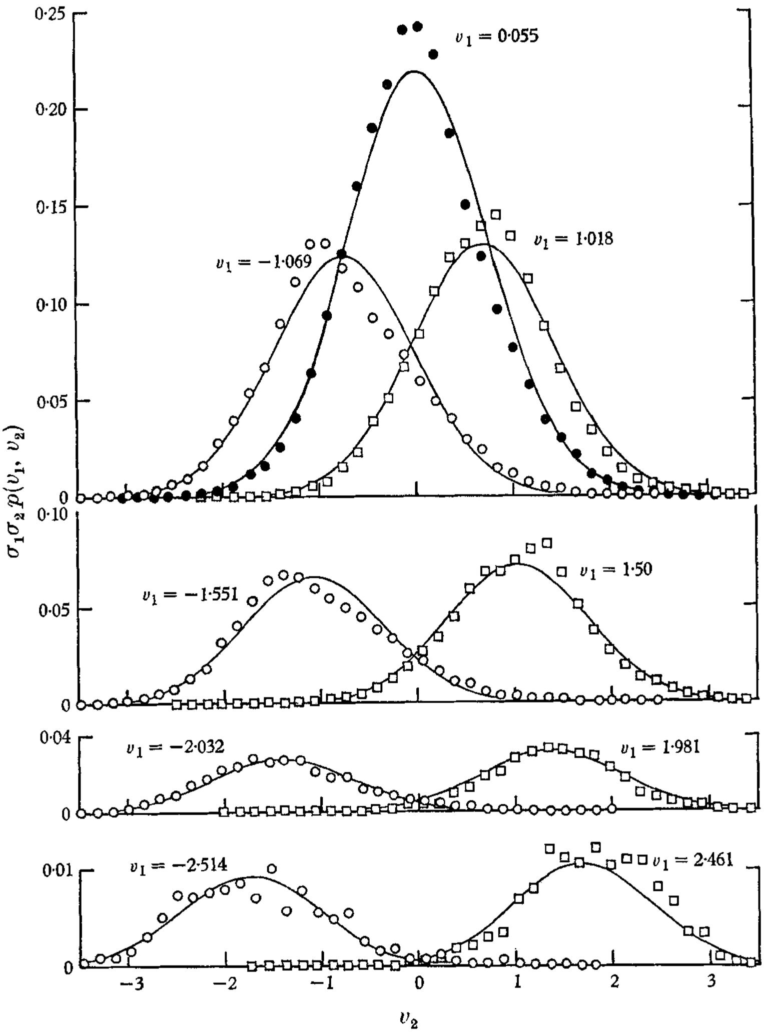

FIGURE 3. Joint probability distribution $p(v_1, v_2)$ for selected values of $v_1 = u(t)/\sigma$. Solid lines are two-dimensional Gaussian distribution corresponding to a correlation coefficient of 0·686.

4. Correlations

4.1. *Computation method*

A series of discrete sequential data samples is customarily referred to as a time series. Cooley & Tukey (1965) have shown that the computationally fastest way to calculate mean lagged products (correlation functions) for a time series is to begin by calculating all Fourier coefficients of the series with a fast-Fourier transform and then to fast-Fourier retransform, a sequence made up of $a_f^2 + b_f^2$, where $a_f + ib_f$ are the complex Fourier coefficients. The fast-Fourier transform is simply an efficient method for computing the discrete Fourier transform. Since calculation of the fast-Fourier transform of a series of N terms requires of the order of $N \log_2 N$ operations, while straightforward calculation of correlations by lagged products requires of the order of N^2 operations, enormous savings in computing time can be realized for the long time series required for turbulence measurements. Both the energy spectrum and autocorrelation are obtained in considerably less time than is required to compute the correlation function alone by direct computation of lagged products. A detailed account of the fast-Fourier discrete transform method has been given by Gentlemen & Sande (1966). Briefly, the discrete transform procedure is as follows: if u_t $(t = 0, 1, 2, \ldots, N-1)$ are the values of a time series, the discrete Fourier transform of the series is

$$\begin{aligned} \mathfrak{U}_f &= \sum_{t=0}^{N-1} u_t \exp(-i2\pi ft/N) \\ &= a_f + ib_f \quad (f = 0, 1, \ldots, N-1), \end{aligned}$$

where the $\mathfrak{U}_f$ are complex Fourier coefficients. The u_t may in general be complex. The discrete transform is equivalent to the Fourier transform of the truncated continuous function (defined over a time interval T) from which the samples of the time series were obtained, namely

$$\mathfrak{U}(f) = \int_{-\frac{1}{2}T}^{\frac{1}{2}T} u(t) \exp(-i2\pi ft)\, dt,$$

where $\mathfrak{U}(f)$ is a complex function of f, and $1/N[a_f^2 + b_f^2]$ is equivalent to the energy spectrum $E(f) = 1/T|\mathfrak{U}(f)|^2$ of the continuous process from which the time series was derived.

The normalized autocorrelation function $R(\tau)$ is defined as

$$R^{1,1}(\tau)\langle u^2 \rangle = R(\tau)\langle u^2 \rangle = \frac{1}{T}\int_{-\frac{1}{2}T}^{\frac{1}{2}T} u^*(t)\, u(t+\tau)\, dt,$$

where * denotes complex conjugate. Letting $t + \tau = y$,

$$\begin{aligned} R(\tau)\langle u^2 \rangle &= \frac{1}{T}\int_{-\frac{1}{2}T}^{\frac{1}{2}T} u(y)\, u^*(y-\tau)\, dy \\ &= \frac{1}{T} u(\tau) \oplus u^*(-\tau), \end{aligned}$$

where $\oplus$ denotes convolution.† Then, from the convolution theorem

$$\begin{aligned} R(\tau)\langle u^2 \rangle &= \frac{1}{T}\mathfrak{F}^{-1}[\mathfrak{U}(f)\,\mathfrak{U}^*(f)] \\ &= \mathfrak{F}^{-1}[E(f)], \end{aligned}$$

where $\mathfrak{F}^{-1}$ denotes the inverse Fourier transform.

The above procedure is readily generalized to the case of two-point correlations of arbitrary order, with the result

$$\langle u^2 \rangle^{\frac{1}{2}(m+n)} R^{m,n}(\tau) = \langle u^m(t)\, u^n(t+\tau) \rangle = \frac{1}{T}\mathfrak{F}^{-1}[\mathfrak{U}_m^*(f)\,\mathfrak{U}_n(f)]$$

† This form of the convolution theorem is discussed by Bracewell (1965).

and $$\langle u^2\rangle^{\frac{1}{2}(m+n)}R^{n,m}(\tau) = \langle u^n(t)\,u^m(t+\tau)\rangle = \frac{1}{T}\mathfrak{F}^{-1}[\mathfrak{U}_m^*(-f)\,\mathfrak{U}_n(-f)],$$

where $\mathfrak{U}_m(f)$ and $\mathfrak{U}_n(f)$ are the complex Fourier transforms of the time series for $u^m(t)$ and $u^n(t)$, respectively. The computing procedure for each correlation is first to compute the discrete Fourier transform $\mathfrak{U}_m(f)$ for each series $u^m(t)$, then to form the products of the complex coefficients of the two series for each frequency, and finally, to compute the inverse discrete Fourier transform of the resulting complex series to obtain $R^{m,n}$. Since the Fourier transform of each series provides values for both positive and negative frequencies in the transform space, both $R^{m,n}(\tau)$ and $R^{n,m}(\tau)$ are obtained from the same fast-Fourier transforms and inverse transforms.

The digital data were Fourier transformed in records containing 2048 digital velocities, the maximum number allowable with the available computer memory. Each record corresponded to a time interval about 20 times longer than the time separation τ required for the double correlations to decay to zero. The number of discrete frequencies in each transform was also chosen as 2048, providing a maximum frequency resolution of 7·82 and 2·74 Hz for the data at high and low speeds, respectively. The appropriate products of the discrete transforms were averaged over 200 and 150 records for the two cases, corresponding to time intervals of 25·6 and 54·9 sec as discussed in §2. These averaged products, each consisting of 2048 complex numbers, were then inverse fast-Fourier transformed to obtain the correlation functions. Since each transformed time series is used several times for different correlations, the relative efficiency of the analysis increases as additional higher-order correlations are computed. The present measurements did not take full advantage of this fact, because available funds made it desirable to restrict the computation to those correlations computed in I and II. For example, to compute $E(f)$, $R^{1,1}(\tau)$, $R^{2,1}(\tau)$ and $R^{1,2}(\tau)$ for a series of 409,600 velocity samples required about 10 min of computer time, while the computation of the other 14 correlations measured required an additional 35 min. Four samples of data for each mean velocity were processed in the above manner, and the resulting correlation functions for the four samples were averaged to produce the final measured correlation functions. As one programme check, several double and triple correlations were also calculated directly from mean lagged products as in I and II. These correlations were in close agreement with the results from the fast-Fourier transform method. Several runs were also made to study the influence of electronic noise by processing sampled data obtained with no grid in the tunnel. The resulting noise correlations, which were dominated mainly by a periodic 60 Hz component, were at most 10^{-4} times as large as the maximum values of the measured triple correlations, indicating that the influence of noise is negligible.

4.2. *Results for even-order correlations*

For all even-order correlations ($m+n$ even), differences between the results of the four individual samples were negligibly small, and a single sample would have been sufficient. The measured correlations for both high and low speeds were generally in very close agreement with the results of Frenkiel & Klebanoff (1967*a*, *b*) for all even-order correlations. The largest differences were found for the double correlation. As shown in figure 4, the results were identical for $U\tau/M \leqslant 1{\cdot}2$.

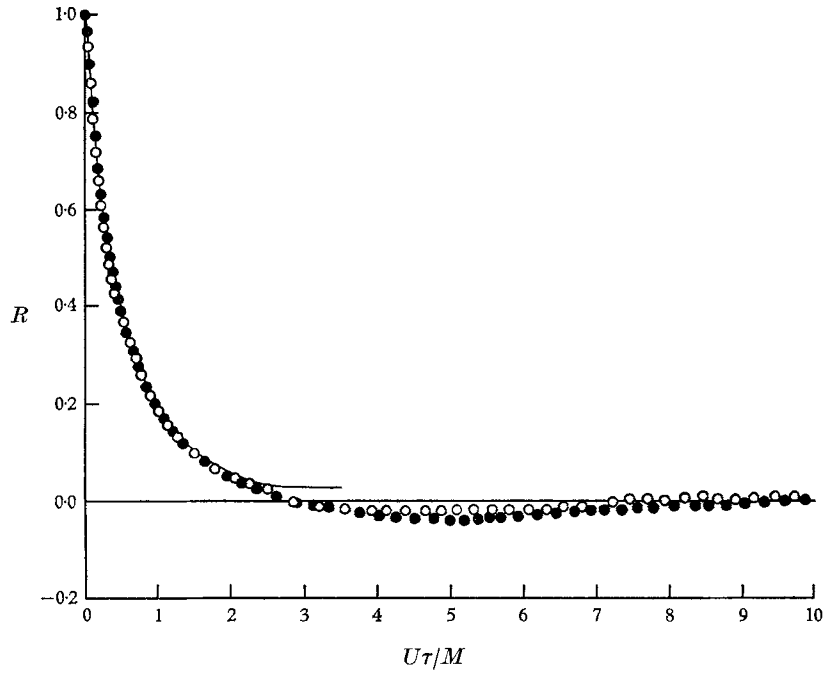

FIGURE 4. Correlation functions. ○, $M = 5{\cdot}08$ cm, $U = 7{\cdot}7$ m/sec; ●, $M = 2{\cdot}54$ cm, $U = 15{\cdot}7$ m/sec; —, Frenkiel & Klebanoff (1967*a*).

However, for $U\tau/M > 1{\cdot}2$ the correlation obtained digitally in I monotonically approaches a small positive value, whereas the present double correlations pass through zero at about $U\tau/M = 2{\cdot}8$, reach a small negative maximum, and then return to zero as $U\tau/M$ further increases. This behaviour is in agreement with the analogue data of Favre, Gaviglio & Dumas (1955), over the entire range of $U\tau/M$. The apparent improvement in resolution of the present digital data for large $U\tau/M$ most probably resulted from using samples of data lasting about twice as long as those employed in I.

The one-dimensional energy spectra E_1, normalized with the Kolmogoroff velocity scale $k_K^{-1}(\epsilon/\nu)^{\frac{1}{2}}$, are plotted in figure 5 as a function of wave-number $k = 2\pi f/U$ normalized with the Kolmogoroff wave-number $k_K = (\epsilon/\nu^3)^{\frac{1}{4}}$. The dissipation rate $\epsilon = -\frac{1}{2}d/dt(\langle u^2\rangle + 2\langle v^2\rangle)$ was computed from the data of figure 1. The Kolmogoroff length scale $(\nu^3/\epsilon)^{\frac{1}{4}}$ was 0·24 and 0·47 mm for the high- and low-speed data, respectively. For clarity, only a few points from the total of 2048 for each spectrum have been plotted. The data for both experimental conditions lie on a single curve, which for large wave-numbers coincides with the universal longitudinal velocity spectrum compiled by Gibson & Schwarz (1963).

The measured higher-order correlations are presented in figures 6–8. For clarity, we have plotted only every third point of the measured correlations, except near $\tau = 0$, where the correlations change rapidly. The same procedure is adopted for the odd-order correlations to follow. Assuming that $r = U\tau$ by Taylor's hypothesis and noting that $R^{m,n}(-\tau) = R^{n,m}(\tau)$, we find that all the

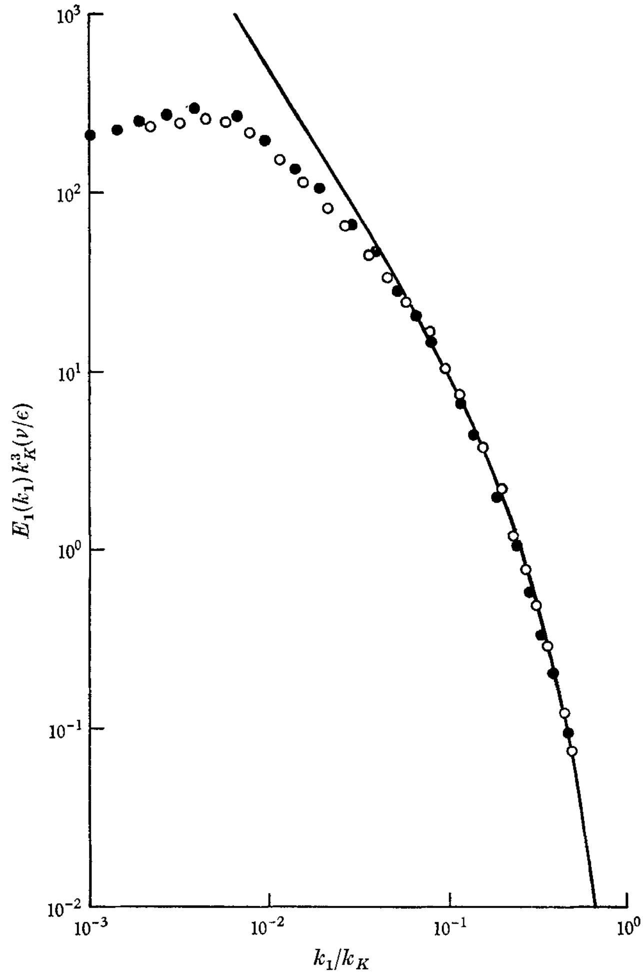

FIGURE 5. Normalized one-dimensional energy spectra. ○, M = 5·08 cm, U = 7·7 m/sec; ●, M = 2·54 cm, U = 15·7 m/sec; solid line is universal velocity spectrum from Gibson & Schwarz (1963).

measured even-order correlations $R^{m,n}$ are symmetrical functions of r. The correlations are in remarkably close agreement with those presented by Frenkiel & Klebanoff (1967*a*), and therefore all flatness factors and other quantities derived from these correlations are also nearly identical with those given in I. Frenkiel & Klebanoff found that even-order correlations closely satisfied the quasi-Gaussian assumption, except for small values of $U\tau/M$. Their conclusions obviously also apply to the present results, which depart from the appropriate Gaussian curves

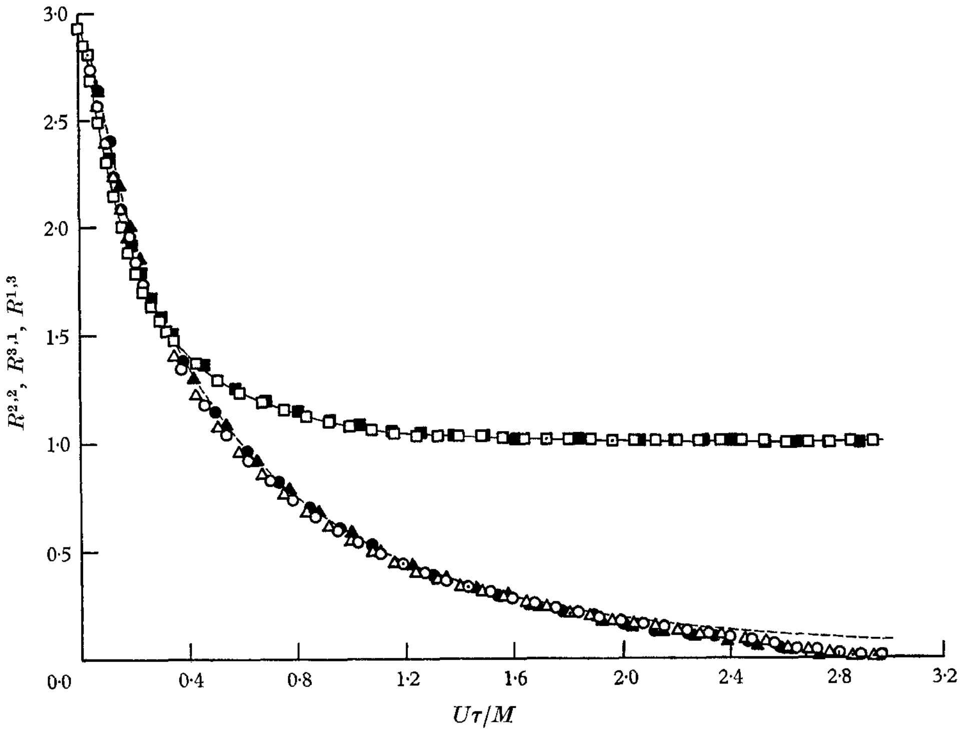

FIGURE 6. Fourth-order correlations. $U = 7{\cdot}7$ m/sec: □, $R^{2,2}$; ○, $R^{3,1}$; △, $R^{1,3}$. $U = 15{\cdot}7$ m/sec: ■, $R^{2,2}$; ●, $R^{3,1}$; ▲, $R^{1,3}$. Solid and dashed curves are from Frenkiel & Klebanoff (1967*a*).

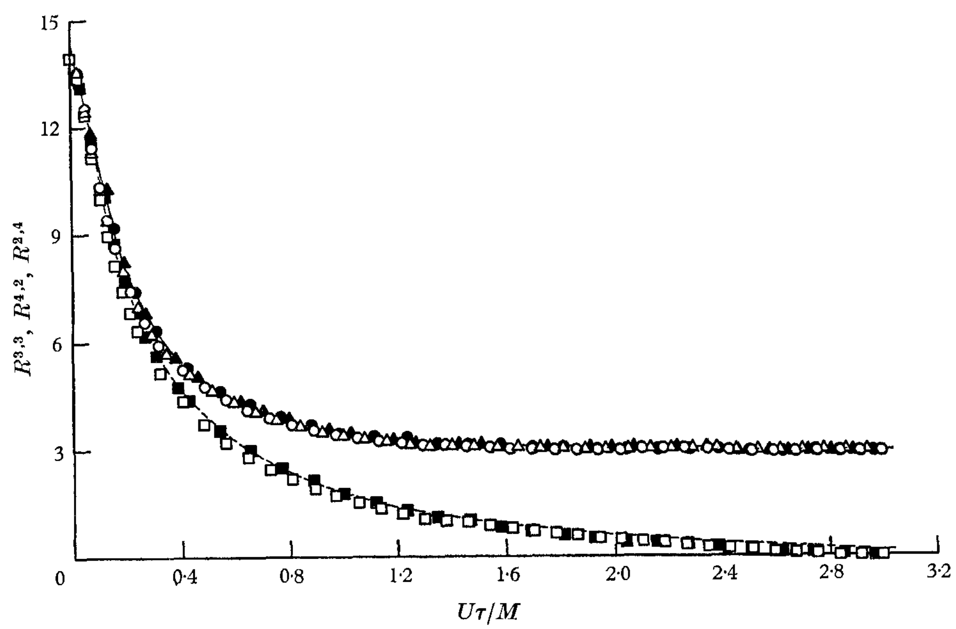

FIGURE 7. Sixth-order correlations. $U = 7{\cdot}7$ m/sec: □, $R^{3,3}$; ○, $R^{3,1}$; △, $R^{2,4}$. $U = 15{\cdot}7$ m/sec: ■, $R^{3,3}$; ●, $R^{4,2}$; ▲, $R^{2,4}$. Solid and dashed curves are from Frenkiel & Klebanoff (1967*a*).

in precisely the same way. As shown in figure 6, the only noticeable deviation from the results of I is a small difference in $R^{3,1}(\tau)$ for $U\tau/M > 1{\cdot}7$. Since the present data required no corrections for non-linear response of the hot wire, the excellent agreement with the results of I provides further confirmation that

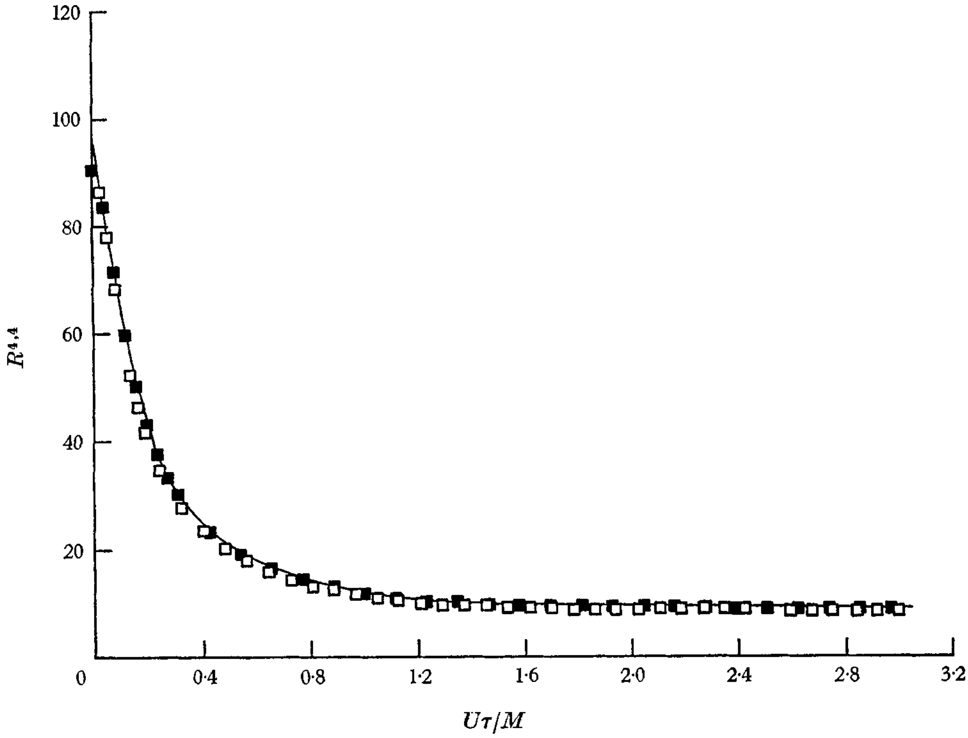

FIGURE 8. Eighth-order correlation $R^{4,4}$. □, $U = 7{\cdot}7$ m/sec; ■, $U = 15{\cdot}7$ m/sec; —, Frenkiel & Klebanoff (1967*a*).

corrections for non-linear response are negligible for even-order correlations and apparently illustrates the power of digital techniques as an accurate tool for turbulence measurements. There is also some evidence, discussed in §4.3, that this agreement reflects a certain gross insensitivity of even-order correlations with regard to certain filtering operations.

4.3. *Results for the odd-order correlations*

Unlike the even-order correlations, the data for the odd-order correlations showed variations between individual samples which increased as the order of the correlations increased. One expects that a larger amount of data will be required to describe odd-order correlations adequately, since they measure small departures from the Gaussian statistics which dominate the even-order correlations. The final measured correlations are therefore not as accurate as for even-order correlations, but the dispersion is sufficiently small that the averages of the four samples are fairly smooth. For the example shown in figure 9 the dispersion in the time skewness $S_t^3 = 3[R^{2,1} - R^{1,2}]$ for the four individual samples is considerably less than in the four samples presented for the same quantity in I as representative of the average of a total of 54 samples. An improvement in the scatter of individual samples is to be expected, as each sample contained nearly four times as many velocities in the present case, but one would expect the present averages over four samples to be somewhat less smooth as about one-third as much total data was used for the final averaged correlations.

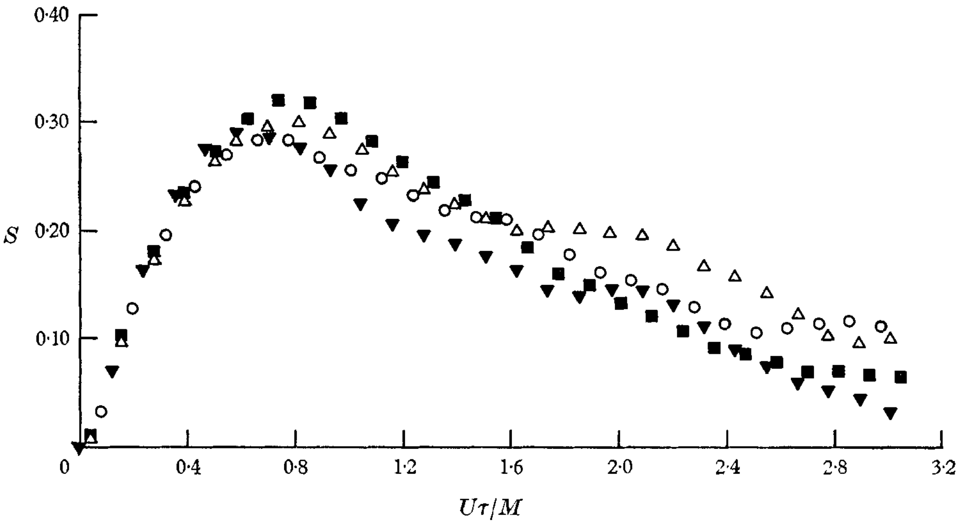

FIGURE 9. Time skewness $S = 3[R^{2,1} - R^{1,2}]$ for four individual samples of data; $M = 2{\cdot}54$ cm, $U = 15{\cdot}7$ m/sec.

For purely isotropic homogeneous turbulence, all two-point odd-order correlations $R^{m,n}(r)$ are antisymmetrical functions of the spatial separation r of the two points. Assuming again that $r = U\tau$ by Taylor's hypothesis and noting that $R^{m,n}(-\tau) = R^{n,m}(\tau)$, we can compare the form of the measured correlations with that expected for true isotropy. For the third-order correlations shown in figure 10, we observe that $R^{2,1}(\tau)$ is a nearly antisymmetrical function of $U\tau/M$, whose negative branch reaches a somewhat larger maximum than is reached for positive $U\tau/M$. The assumption of isotropy therefore appears reasonably adequate for the third-order correlations downstream of a grid. The opposite conclusion has been reached by Frenkiel & Klebanoff, who found $R^{2,1}(0) = 0{\cdot}05$ and a maximum value of $R^{2,1}(\tau)$ of about 0·057. Fifth- and seventh-order correlations are plotted in figures 11–13. None of the correlations is perfectly antisymmetrical with respect to $U\tau/M$, but they show a strong tendency toward antisymmetry, and the correlations are strikingly different from those reported in I and II. Except for $R^{3,2}(\tau)$, the magnitude of the correlations for negative $U\tau/M$ is consistently somewhat larger than for positive $U\tau/M$. Apart from this systematic behaviour, the assumption of isotropy appears to be qualitatively satisfied. One notes from the increasing undulations in the curves that even the substantial amount of data used in the present measurements becomes increasingly less adequate as both the order of the correlations and $U\tau/M$ increase.

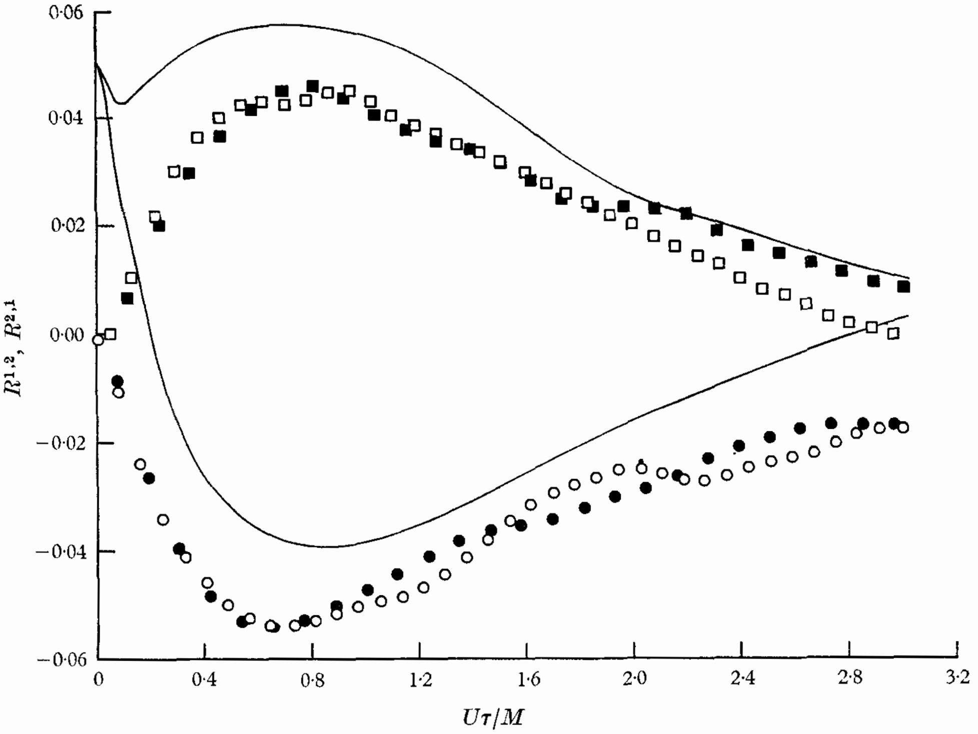

FIGURE 10. Triple correlations. $M = 5{\cdot}08$ cm, $U = 7{\cdot}7$ m/sec: □, $R^{2,1}$; ○, $R^{1,2}$. $M = 2{\cdot}54$ cm, $U = 15{\cdot}7$ m/sec: ■, $R^{2,1}$; ●, $R^{1,2}$. —, Frenkiel & Klebanoff (1967*a*).

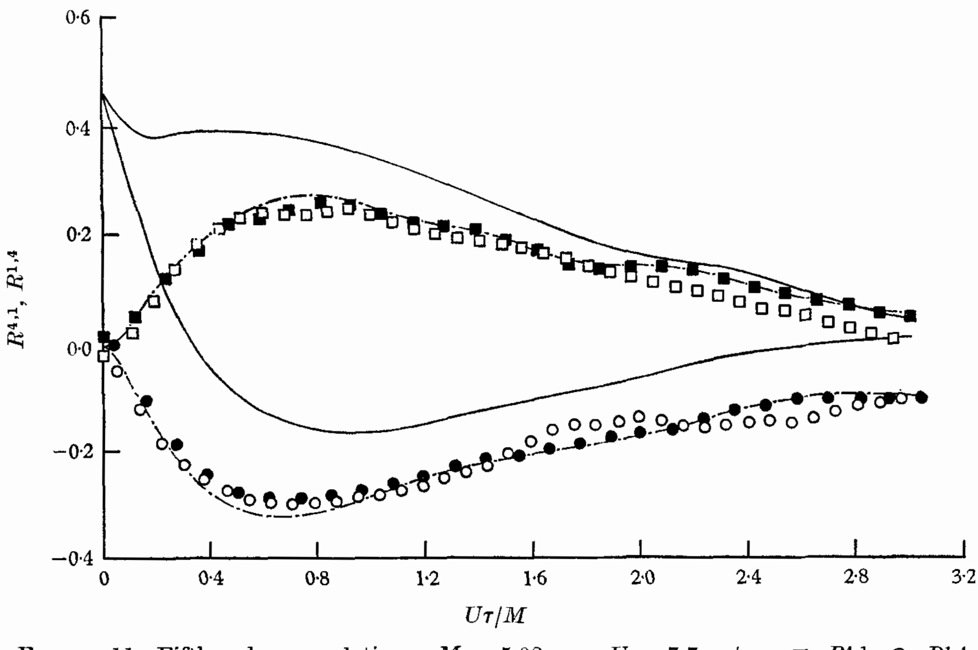

FIGURE 11. Fifth-order correlations. $M = 5{\cdot}08$ cm, $U = 7{\cdot}7$ m/sec: □, $R^{4,1}$; ○, $R^{1,4}$. $M = 2{\cdot}54$ cm, $U = 15{\cdot}7$ m/sec: ■, $R^{4,1}$; ●, $R^{1,4}$. Solid lines are data of Frenkiel & Klebanoff (1967*b*). Dashed lines obtained from present measured second- and third-order correlations ($M = 2{\cdot}54$ cm, $U = 15{\cdot}7$ m/sec) using fourth-order non-Gaussian probability density.

The present odd-order correlations are in clear disagreement with those of I and II. We have so far been able to deduce no entirely satisfactory explanation for these differences. There is, however, some experimental evidence that appears to be particularly relevant. The effect of using a high-pass filter to eliminate the d.c. level was briefly investigated in some preliminary attempts to digitize the present data. Correlations up to third-order were measured with and without the

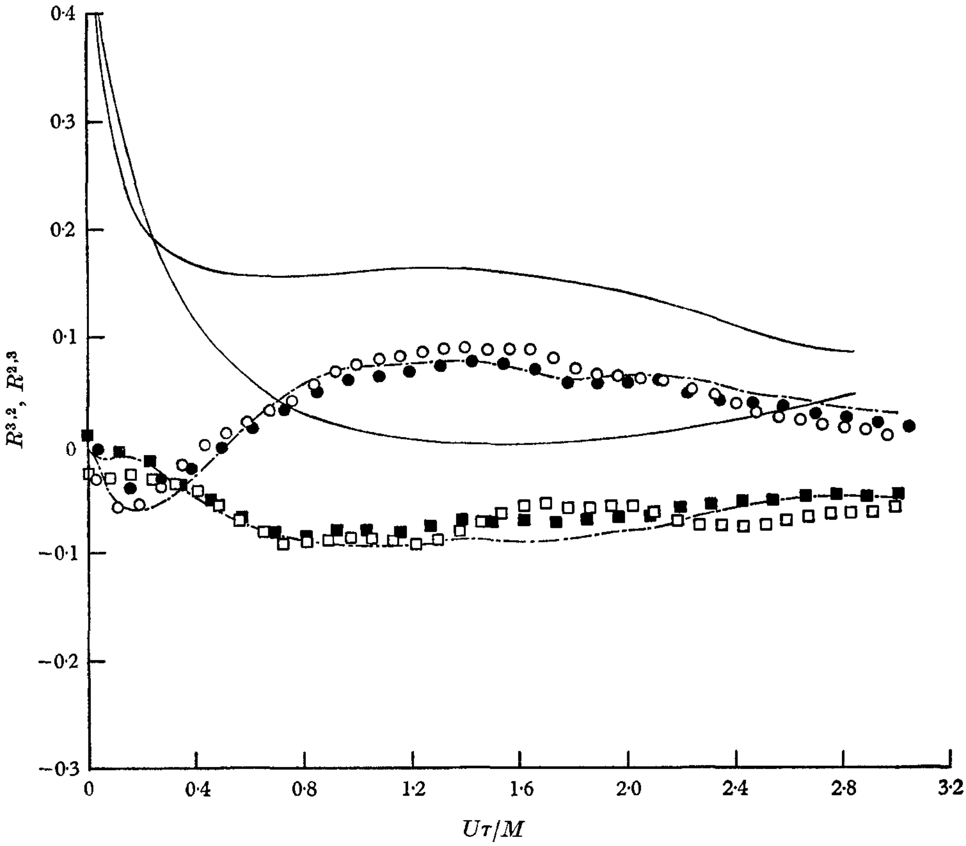

FIGURE 12. Fifth-order correlations. $M = 5{\cdot}08$ cm, $U = 7{\cdot}7$ m/sec: □, $R^{3,2}$; ○, $R^{2,3}$. $M = 2{\cdot}54$ cm, $U = 15{\cdot}7$ m/sec: ■, $R^{3,2}$; ●, $R^{2,3}$. Solid lines are data of Frenkiel & Klebanoff (1967*b*). Dashed lines obtained from present measured second- and third-order correlations ($M = 2{\cdot}54$ cm, $U = 15{\cdot}7$ m/sec) using fourth-order non-Gaussian probability density.

filter. While the double correlation was practically unaffected by filtering, the triple correlations were substantially different for the two cases. As shown in figure 14, high-pass filtering (Kronhite 335-M filter with cut-off set at 1·9 Hz) changed the $\langle u^3 \rangle$ from a nearly zero value to a positive value close to that reported in II, and the entire triple correlation curves closely resemble those reported in II. Noting that the compensated hot-wire amplifier used in I and II was a.c. coupled and had low-frequency attenuation and phase-shift characteristics

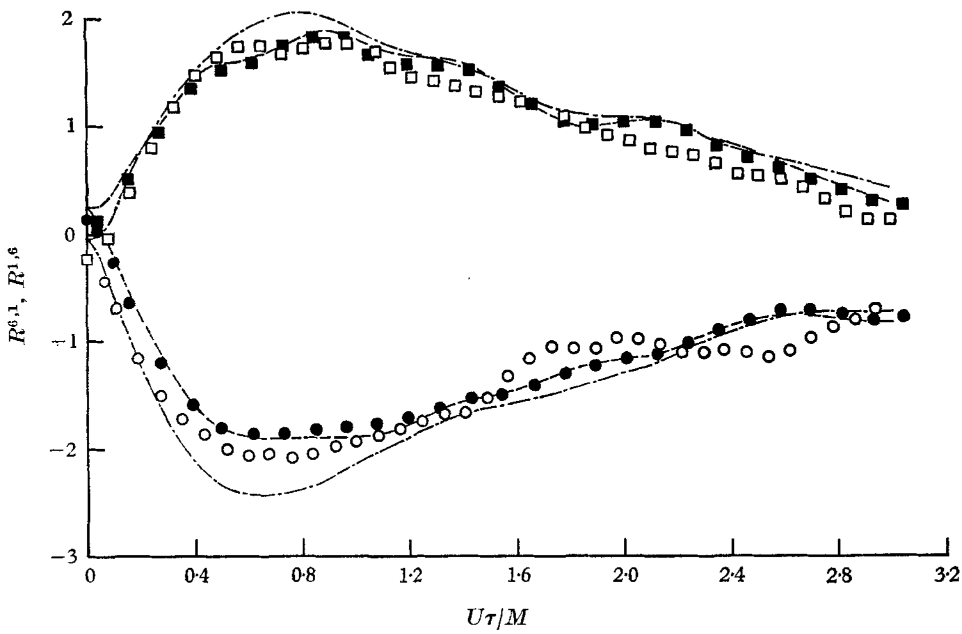

FIGURE 13. Seventh-order correlations. M = 5·08 cm, U = 7·7 m/sec: □, $R^{6,1}$; ○, $R^{1,6}$. M = 2·54 cm, U = 15·7 m/sec: ■, $R^{6,1}$; ●, $R^{1,6}$. ·—·, obtained from measured second- and third-order correlations (M = 2·54 cm, U = 15·7 m/sec) using fourth-order non-Gaussian probability density. – – –, obtained from measured second-, third- and fifth-order correlations (M = 2·54 cm, U = 15·7 m/sec) using sixth-order non-Gaussian probability density.

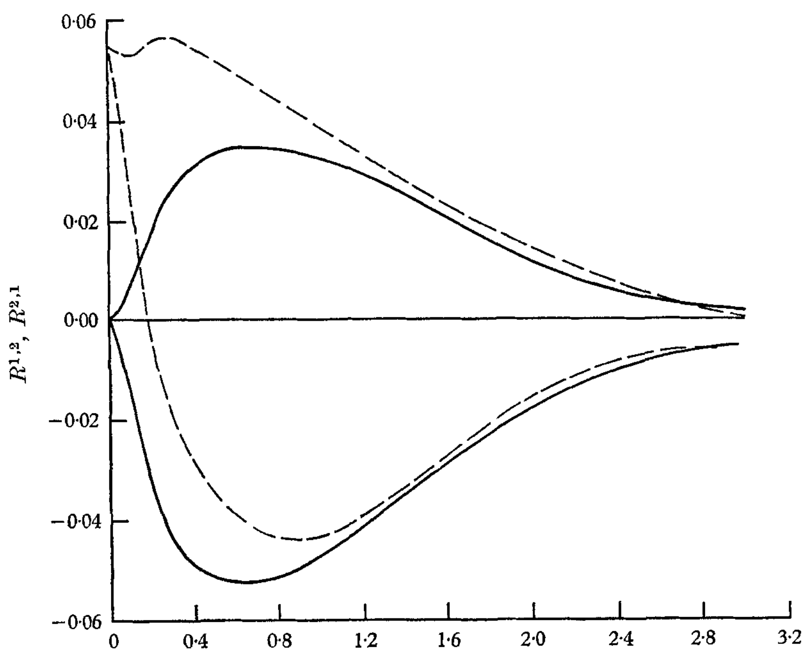

FIGURE 14. Effect of high-pass filter on measured triple correlations. Solid lines are preliminary data obtained without filter, dashed lines are preliminary data obtained using high-pass filter.

similar to our high-pass filter,† the non-zero values of $\langle u^3 \rangle$ (and quite likely higher odd powers of u) observed in I and II may have been due to the effects of filtering on low-frequency velocity fluctuations. In support of this hypothesis, we note that the unpublished measurements of Harris and Corrsin cited in II as agreeing with the data of II with respect to the non-zero value of skewness and the form of the triple correlations also were obtained using a high-pass filter after the linearizer to eliminate the d.c. level.‡ For all the data presented earlier in the present paper the d.c. level was removed simply by subtracting the mean value from each sampled velocity and the high-pass filter was not used. The possible significance of our preliminary (incorrect) filtered data with respect to other previous measurements was not fully appreciated during our preliminary measurements and other higher correlations were not determined using the

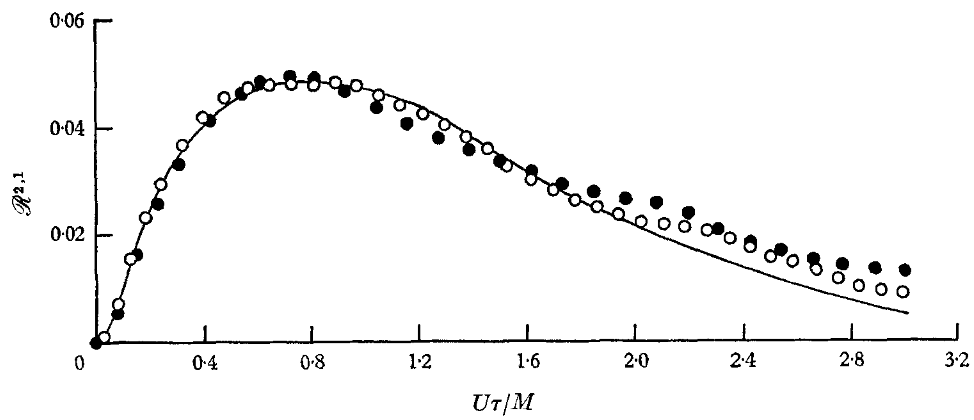

FIGURE 15. Composite third-order correlation $\mathscr{R}^{2,1}$. ○, M = 5·08 cm, U = 7·7 m/sec; ●, M = 2·54 cm, U = 15·7 m/sec. Solid curve is from Frenkiel & Klebanoff (1967*b*).

filtered data. However, it appears quite likely from the above discussion that the non-zero values of $\langle u^5 \rangle$ and $\langle u^7 \rangle$, and the accompanying severe non-symmetry of the corresponding odd-order correlations reported in I and II were also caused by inadvertent high-pass filtering. If this is indeed the case, then the even-order correlations, which apparently were not noticeably affected, must be relatively insensitive to such a filtering operation. An analytical description of the effects of high-pass filtering on measuremements of higher moments of non-Gaussian processes would be a useful contribution at this point.

Despite the large differences in individual correlations, all differences of correlations defined as $\mathscr{R}^{m,n} = \frac{1}{2}(R^{m,n} - R^{n,m})$ by Frenkiel & Klebanoff are found to be very close to the results given in I, as shown in figures 15–17. For small values of $U\tau/M$, near agreement is inevitable since the $\mathscr{R}^{m,n}$ are required by definition to be zero at $U\tau/M = 0$, but the agreement is fairly good over the entire range of $U\tau/M$. It appears that the $\mathscr{R}^{m,n}$ are rather insensitive to the exact form of the

† P. S. Klebanoff, private communication.

‡ S. Corrsin, private communication.

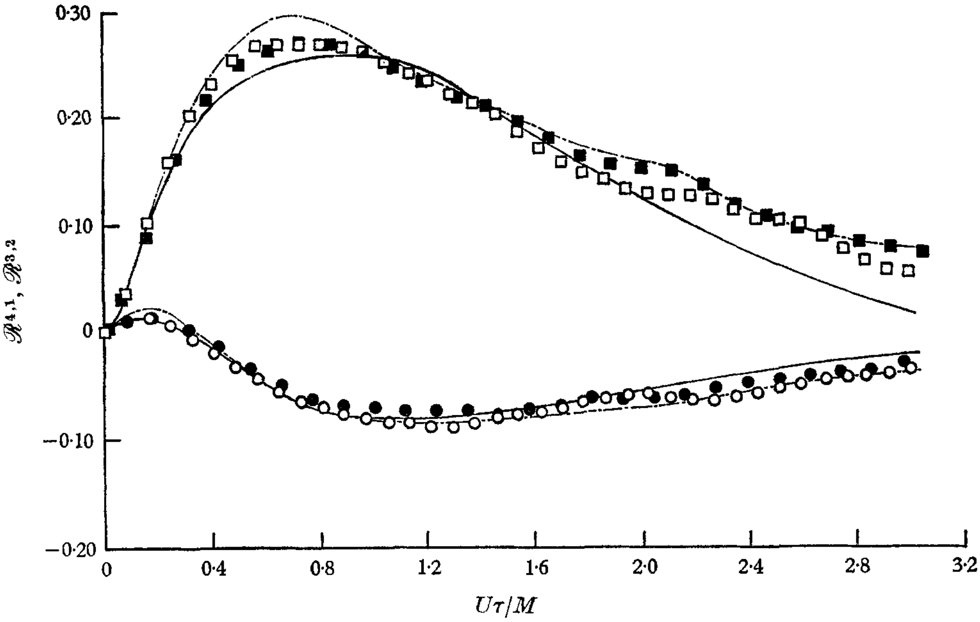

FIGURE 16. Composite fifth-order correlations. $M = 5{\cdot}08$ cm, $U = 7{\cdot}7$ m/sec: □, $\mathscr{R}^{4,1}$; ○, $\mathscr{R}^{3,2}$. $M = 2{\cdot}54$ cm, $U = 15{\cdot}7$ m/sec: ■, $\mathscr{R}^{4,1}$; ●, $\mathscr{R}^{3,2}$. Solid curves are from Frenkiel & Klebanoff (1967*a*). ·—·, $M = 2{\cdot}54$ cm, $U = 15{\cdot}7$ m/sec, obtained by using fourth-order non-Gaussian probability density.

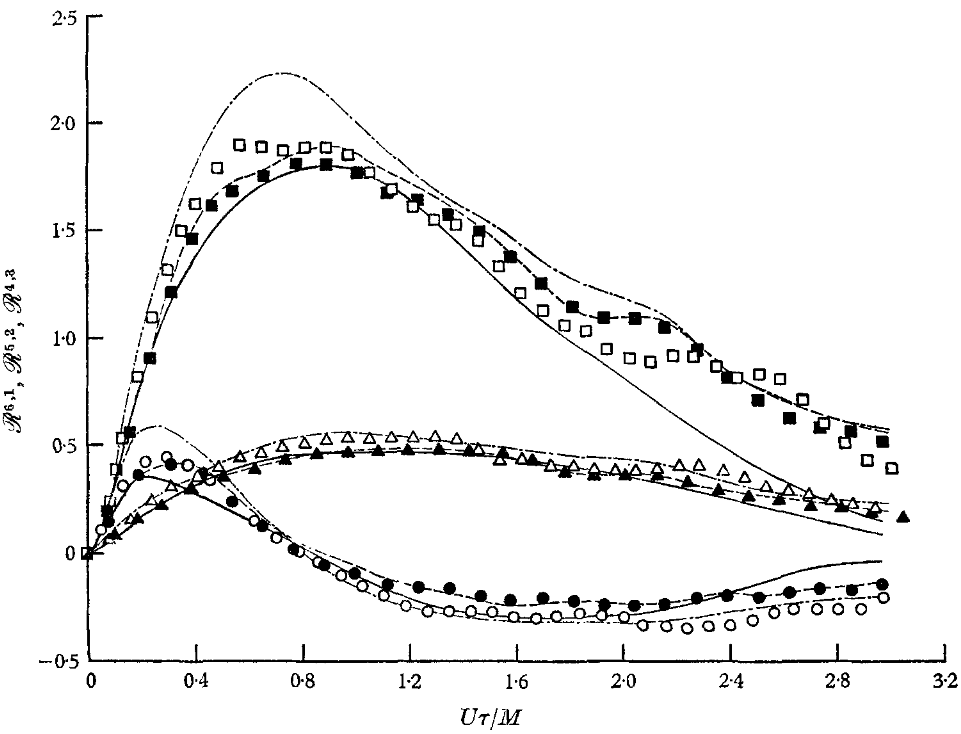

FIGURE 17. Composite seventh-order correlations. $M = 5{\cdot}08$ cm, $U = 7{\cdot}7$ m/sec: □, $\mathscr{R}^{6,1}$; ○, $\mathscr{R}^{5,2}$; △, $\mathscr{R}^{4,3}$. $M = 2{\cdot}54$ cm, $U = 15{\cdot}7$ m/sec: ■, $\mathscr{R}^{6,1}$; ●, $\mathscr{R}^{5,2}$; ▲, $\mathscr{R}^{4,3}$. Solid curves are from Frenkiel & Klebanoff (1967*a*). ·—· and – – –, $M = 2{\cdot}54$ cm, $U = 15{\cdot}7$ m/sec, obtained by using fourth- and sixth-order non-Gaussian probability densities, respectively.

correlations, and hence are not a discriminating measure of turbulent structure, especially for small values of $U\tau/M$.

Since all the odd-order correlations would be zero if the joint probability density function for the fluctuating velocity were Gaussian, it is of interest to investigate the usefulness of non-Gaussian distributions in representing relations between odd-order moments. We have done this using the Gram–Charlier joint probability distribution described in detail in I and find that this distribution describes relations between the individual $R^{m,n}$ correlations (and hence between the $\mathscr{R}^{m,n}$ as shown previously in I) remarkably well. Comparison of individual and composite ($\mathscr{R}^{m,n}$) correlations with predictions from lower-order correlations using relations given in I are shown in figures 15–17. These comparisons verify (as discussed in I) that the fourth-order non-Gaussian distribution appears to be adequate for describing fifth-order correlations in terms of lower-order ones, while a sixth-order distribution is needed to provide a good fit for the seventh-order correlations. In view of the apparent success of the Gram–Charlier distribution in representing relations between odd-order correlations, it is unfortunate that a probability distribution function of this type has the pathological property of producing negative values for some parts of the distribution function.

5. Conclusions

The assumptions of isotropy appear to be qualitatively satisfied by the present measured odd-order correlations, in contrast with previous measurements by other investigators. The present data for higher-order correlations may therefore prove useful for quantitative comparison with corresponding theoretical predictions for isotropic turbulence, when these become available. Differences in the low-frequency response of hot-wire amplifiers and associated instruments may account for the differences between the present data for odd-order correlations and that of earlier investigators. The present even-order correlations are generally in excellent agreement with previous measurements and, except for very small values of the time separation, higher correlations may be accurately predicted from a knowledge of only the second-order correlation by assuming a Gaussian joint probability density for fluctuations in velocity at different times. Digital harmonic analysis employing the fast-Fourier transform provides a powerful and efficient technique for measuring two-point correlations of arbitrary order in turbulent flows.

We wish to thank Mr Granger Morgan of the UCSD Department of Applied Electrophysics for his invaluable help in digitizing the data and for suggestions concerning the analysis. The work was supported principally by the National Science Foundation, Grant GK-1515; and partially by the Advanced Research Projects Agency (Project DEFENDER) through Contract no. DA-31-124-ARO-D-257 monitored by the U.S. Army Research Office, Durham.

REFERENCES

Bracewell, R. 1965 *The Fourier Transform and its applications.* New York: McGraw-Hill.

Comte-Bellot, G. & Corrsin, S. 1966 *J. Fluid Mech.* **25**, 657.

Cooley, J. W. & Tukey, J. W. 1965 *Math. Comput.* **19**, 297.

Favre, A., Gaviglio, J. & Dumas, R. 1955 Some measurements of time and space correlation in wind tunnel. *NACA TM* 1370.

Frenkiel, F. N. & Klebanoff, P. S. 1965 *Phys. Fluids*, **8**, 2291.

Frenkiel, F. N. & Klebanoff, P. S. 1967*a* *Phys. Fluids*, **10**, 507.

Frenkiel, F. N. & Klebanoff, P. S. 1967*b* *Phys. Fluids*, **10**, 1737.

Gentleman, W. M. & Sande, G. 1966 *Fall Joint Computer Conference, AFIPS Proc.* **29**, 563.

Gibson, C. H. & Schwarz, W. H. 1963 *J. Fluid Mech.* **16**, 365.